A unique polarized x-ray facility at the Advanced Photon Source

J. W. Freeland,[a] J. C. Lang, G. Srajer, R. Winarski, D. Shu, and D. M. Mills
Advanced Photon Source, Argonne National Laboratory, Argonne, Illinois 60439

(Presented on 22 August 2001)

To use the unique element-specific nature of polarized x-ray techniques to study a wide variety of problems related to magnetic materials, we have developed a dual-branch sector that simultaneously provides both hard and soft x-ray capabilities. This facility, which is located in sector 4, is equipped with two different insertion devices providing photons in both the intermediate (0.5–3 keV) and hard x-ray regions (3–100 keV). This facility is designed to allow the simultaneous branching of two undulator beams generated in the same straight section of the ring. © *2002 American Institute of Physics.* [DOI: 10.1063/1.1435814]

I. INTRODUCTION

The production of high-intensity polarized x rays at third-generation light sources has led to the development of many new types of polarization-modulated x-ray diffraction and spectroscopy techniques. Research in magnetic materials has particularly benefited from these new techniques, where polarized x rays provide unique information not readily available via other methods.[1] In particular, the importance of photon helicity in spin-dependent magnetic interaction has led to an increased demand for high-quality circularly polarized x-ray sources. Sector 4 of the Advanced Photon Source (APS) has been developed to provide such capabilities. This sector is designed with two branch lines each with its own insertion device. A unique feature of this facility is that, although both insertion devices are placed in the same straight section of the storage ring, they are oriented such that each can be used simultaneously without affecting the operation of the other branch. Furthermore, one insertion device has been designed to produce x rays at intermediate energies (0.5–3 keV), while the other produces x rays at hard x-ray energies (3–100 keV). Therefore, this facility offers the ability to examine the same sample over a wide energy range. As of August 2001, the construction of both branch lines is complete and commissioning activities are in progress.

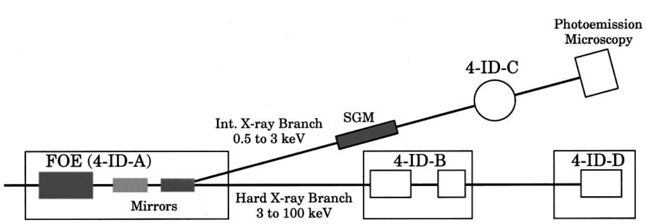

FIG. 1. Layout of sector 4 showing both intermediate and hard x-ray branchlines. FOE—first optics enclosure; and SGM—spherical grating monochromator.

II. SECTOR LAYOUT

The layout of the APS sector 4 polarized x-ray facility is shown in Fig. 1. The beams from each insertion device enter the first optics enclosure (FOE) where a set of horizontal mirrors is used to separate the intermediate (4-ID-C) and the hard (4-ID-D) x-ray branch lines. The insertion device for the intermediate range is a fully electromagnetic undulator. This device is a circularly polarizing undulator (CPU) that can provide left or right circular, as well as horizontal- and vertical-linear, polarization states (see Table I for parameters).[2] The insertion device for the hard x-ray branch is a standard APS undulator A (see Table II for parameters).[3] This device produces horizontally polarized hard x rays in the plane of the orbit, which are subsequently converted to circular polarization through the use of phase retarding optics (see Sec. IV).

In order to separate the beams originating from the hard and soft x-ray undulators, the axes of the undulators are canted as depicted in Fig. 2. The electron beam is first deviated by 135 μradians towards the center of the ring by a

TABLE I. Source parameters of the CPU.

Period	12.8 cm
Number of vertical poles	35
Number of horizontal poles	36
Length	2.4 m
Vertical pole gap	8 mm
Maximum magnetic field	0.24 T
First harmonic energy range	0.5–3 keV
Electromagnet dc stability	<1%
Total power	800 W

TABLE II. Source parameters of the undulator A.

Period	3.3 cm
Number of periods	72
Length	2.4 m
Minimum gap	11 mm
Maximum K	2.77
Minimum first harmonic	2.92 keV
Maximum field	0.899 T
Total power	6.0 kW

[a]Electronic mail: freeland@anl.gov

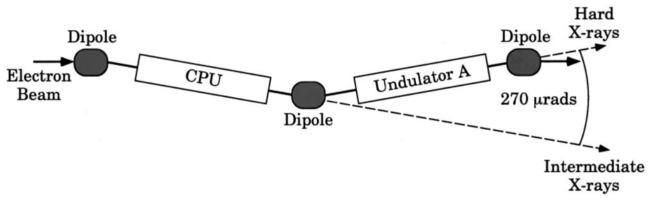

FIG. 2. Canted orientation of sector 4 undulators. CPU—circularly polarizing undulator.

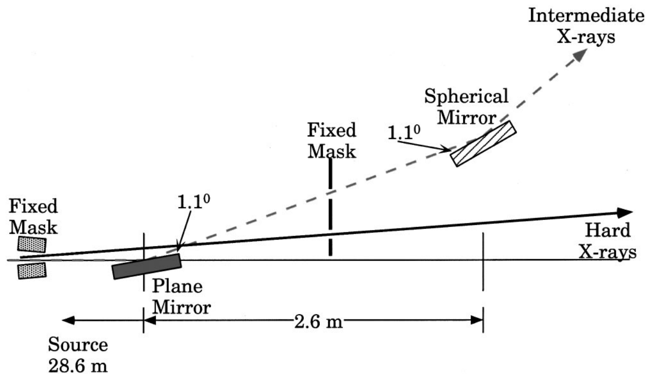

FIG. 3. Schematics of the optics for additional beam deflection in the first optics enclosure (FOE).

fixed dipole magnet before traversing the CPU. After the CPU, a second dipole deflects the beam outward by 270 μradians before entering the undulator A. A third dipole magnet then returns the beam to the normal orbit. These deviations provide a 270 μradian splitting of the two x-ray beams. At 30 m from the source, this separates the beams by 8 mm, which provides sufficient room for optics to capture and separate the beams.

The optics for additional beam deflection are contained in the FOE, as shown in Fig. 3. The first element in the FOE is the fixed mask that reduces unwanted power in the beam and selects out the central cone of the first harmonic. After the second fixed mask, the hard x-ray beam travels straight through the FOE and down to the first experimental hutch described in Sec. IV. The intermediate x rays are reflected though a set of two horizontal mirrors to increase the beam separation and direct the beam outward into the intermediate x-ray beamline (see Sec. III). In order to preserve the polarization of the beam and maintain high reflectivity up to 3 keV with only simple mirror coatings (Rh in this case), an incident angle of 1.1° is used. The first mirror has a plane figure, while the second is spherical with a radius of 1610 m determined by the distance to the first end station (31 m). Both mirrors are made out of Si with cooling provided by Cu side clamps.[4] Since the power in the CPU is low (640 W) and the footprint is large (200 mm), the power density is reduced to a level where this type of cooling is adequate.

III. INTERMEDIATE X-RAY BEAMLINE

Once the horizontal mirrors system has directed the x-ray beam into the intermediate x-ray branch (beamline 4-ID-C), the x ray passes through a spherical grating monochromator (SGM) before arriving at the end stations. The

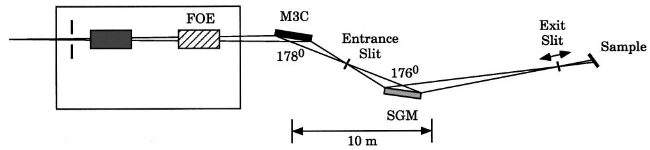

FIG. 4. Intermediate x-ray beamline (sideview).

optics are shown in Fig. 4 and described in more detail elsewhere.[5] This system was previously in operation in sector 2 of the APS. The beamline is designed to provide high-resolution photons for spectroscopy in the 0.5 to 3 keV region. At a resolving power of 5000 at 1 keV, the flux is $\sim 10^{12}$ photons/s delivered into a $0.2(v)\times 2(h)$ mm spot. Initial measurements of the circular polarization, p_c, using the magnetic circular dichroism of standard samples, indicate that $p_c > 96\%$.

Currently, the beamline is equipped with two end stations: one for field- and temperature-dependent absorption, and the second for photoemission microscopy (PEEM). Absorption in the first station can be measured both by total electron yield and partial fluorescence yield using an energy-discriminating Ge/detector. With the sample situated at the end of a liquid He flow cryostat in the poles of an *in situ* electromagnet, the temperature can be controlled from 30 to 450 K in magnetic fields up to 1 kOe. The second station is a commercially built PEEM with integral sample stage from Omicron Associates.

IV. HARD X-RAY BEAMLINE

A schematic of the optical layout for the hard x-ray branch (beamline 4-ID-D) is shown in Fig. 5. All optical components for this beamline are located in the second optics enclosure (4-ID-B) indicated in Fig. 1. The optics consist of a set of tungsten slits, a double-crystal monochromator, two phase-retarding crystals, and two mirrors. The phase retarders or mirrors can be removed from the beam depending on the experimental requirements.

The monochromator for the hard x-ray branch is a fixed exit beam design where the energy is chosen by rotating about an axis through the first crystal and adjusting the position of the second crystal to maintain a fixed exit beam. The offset height between the monochromatic and white beam is variable between 10 and 35 mm. Using Si (111) crystals, the energy range that can be covered is 2 to 45 keV with a resolution of $\Delta E/E$ 1.4×10^{-4}. Other crystals can be used to extend the energy range of the monochromator up to 100 keV. Both crystals of the monochromator are cryogeni-

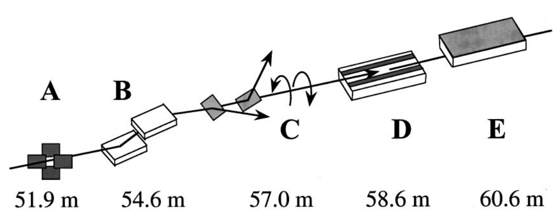

FIG. 5. Layout and distance from the source of the major optical components of the hard x-ray branch. (a) Slits, (b) double-crystal monochromator, (c) phase retarders, (d) focusing mirror, and (e) flat mirror.

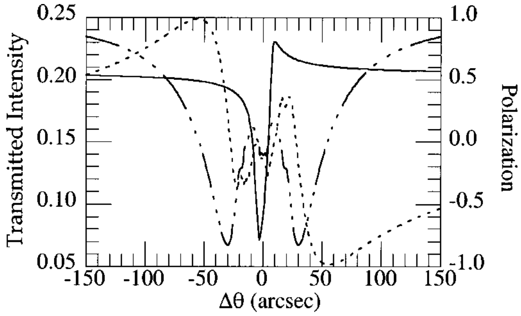

FIG. 6. Calculated intensity (solid) and the linear (dashed) and circular (dotted) polarizations vs deviation from the Bragg angle for the beam transmitted through a 400-μm-thick (111) diamond at 8 keV.

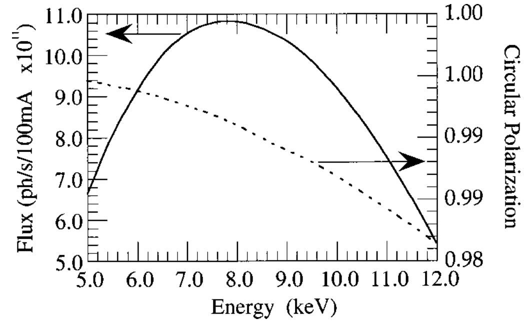

FIG. 7. Flux and circular polarization rate expected for the first harmonic of the undulator after transmission through the diamond phase retarder.

cally cooled with liquid nitrogen, to dissipate the heat of the x-ray beam and maintain an equal lattice spacing.

A unique element of the optical design of this beamline is the manipulation of the polarization of the x-ray beam using phase-retarding crystals.[6] In this optic, the x-ray beam is transmitted through a thin crystal oriented near a Bragg reflection. The wave fields inside a crystal propagate with different phase velocities for different linear directions of polarization. This results in a phase difference, δ, which is related to the degree of linear and circular polarization in the transmitted beam by

$$P_{\mathrm{lin}}=\frac{2\sqrt{I_{\perp}I_{\parallel}}}{I_{\perp}+I_{\parallel}}\cos\delta, \quad P_{\mathrm{circ}}=\frac{2\sqrt{I_{\perp}I_{\parallel}}}{I_{\perp}+I_{\parallel}}\sin\delta, \tag{1}$$

where $I_{\parallel}$ and $I_{\perp}$ are the intensities of the polarization components in and out of the diffraction plane. To get a circularly polarized beam, these intensities must be the same, and δ must be equal to $\pi/2$. Equal intensities can be obtained by inclining the diffraction plane of the phase retarder at 45° with respect to linear polarization of the incoming beam. The phase difference is a function of the deviation from the Bragg condition for the reflection, $\Delta\theta$. Therefore, the polarization of the transmitted beam can be controlled by adjusting $\Delta\theta$. Figure 6 shows calculated values for the variation in the polarization of the beam transmitted through a 400-μm-thick diamond (111) crystal at 8 keV as a function of $\Delta\theta$. Several phase-retarding crystals of different thickness are used to cover the energy range from 5 to 12 keV.

The phase-retarder setup is followed by a 0.8-m-long palladium coated focusing mirror. This mirror has an adjustable curvature along the beam direction (∞ to 6 km) to focus the beam vertically. There are also two grooves with fixed radii of 80 and 345 mm transverse to the beam for horizontal focusing. The 80 mm groove nominally focuses the beam at the center of the experimental station (75 m from the source) for a 3 mrad incident angle, while the 345 mm groove is used to collimate the beam. The focal spot from the mirror is expected to be $\sim$300 μm$\times$100 μm. The beam reflected off the first mirror can enter the experimental station for angles up to 3.7 mrad. For higher incident angles (and to have a horizontal beam in the experimental station), a second 0.8-m-long palladium coated flat mirror can be used.

Figure 7 shows the expected circularly polarized flux for the first harmonic in the experimental station using the phase retarder. If circular polarization is not required, the phase retarder can be removed, and the flux will increase by approximately a factor of 5.

In conclusion, the combination of wide energy range with polarization control make this facility a unique and valuable resource to the experimental community.

ACKNOWLEDGMENTS

Use of the APS was supported by the U.S. Department of Energy, Office of Science, under Contract No. W-31-109-ENG-38.

[1] J. B. Kortright, D. D. Awschalom, J. Stöhr, S. D. Bader, Y. U. Idzerda, S. S. P. Parkin, I. K. Schuller, and H.-C. Siegmann, J. Magn. Magn. Mater. **207**, 7 (1999).
[2] E. Gluskin *et al.*, AIP Conf. Proc. **521**, 344 (2000).
[3] R. J. Dejus, B. Lai, L. R. Moog, and E. Gluskin, Argonne National Laboratory Report No. ANL/APS/TB-17 (1993).
[4] A. M. Khounsary and W. Yun, Rev. Sci. Instrum. **67**, 3354 (1996).
[5] K. J. Randall, E. Gluskin, and Z. Xu, Rev. Sci. Instrum. **66**, 4081 (1995).
[6] J. C. Lang and G. Srajer, Rev. Sci. Instrum. **66**, 1540 (1995).